

# Time-domain stabilization of carrier-envelope phase in femtosecond light pulses

Young-Jin Kim,<sup>1,2,\*</sup> Ian Coddington,<sup>1</sup> William C. Swann,<sup>1</sup> Nathan R. Newbury,<sup>1</sup>  
Joohyung Lee,<sup>2</sup> Seungchul Kim,<sup>2</sup> and Seung-Woo Kim<sup>2</sup>

<sup>1</sup>National Institute of Standards and Technology, 325 Broadway, Boulder CO 80305 USA  
<sup>2</sup>Ultrafast Optics for Ultraprecision Group, KAIST Institute for Optical Science and Technology, Korea Advanced Institute of Science and Technology (KAIST), Science Town, Daejeon, 305-701, South Korea  
[yj.kim@kaist.ac.kr](mailto:yj.kim@kaist.ac.kr)

**Abstract:** We report a time-domain method of stabilizing the carrier-envelope phase (CEP) of femtosecond pulses. Temporal variations of the pulse envelope and the carrier electric-field phase were separately detected with the aid of intensity cross-correlation and interferometric cross-correlation. These detected signals were used to stabilize the CEP; the resulting 50-fold improvement in the fractional stability of the carrier-envelope-offset frequency was evaluated as  $1.2 \times 10^{-11}$  at 0.1 second averaging periods and  $1.7 \times 10^{-9}$  at 80 seconds, corresponding to a carrier envelope phase noise of 75 microradians and 10 milliradians, respectively. This method can be realized with a low pulse energy of  $\sim 10$  pJ and does not require subsequent power amplification or spectral broadening. The high efficiency and short-term stability of this method can facilitate the use of femtosecond lasers in the field of industrial surface measurements, telecommunications, and space sciences.

©2014 Optical Society of America

**OCIS codes:** (140.3425) Laser stabilization; (140.4050) Mode-locked lasers; (120.3930) Metrological instrumentation; (120.4800) Optical standards and testing; (120.3940) Metrology.

---

## References and links

1. T. Udem, R. Holzwarth, and T. W. Hänsch, "Optical frequency metrology," *Nature* **416**(6877), 233–237 (2002).
2. D. J. Jones, S. A. Diddams, J. K. Ranka, A. Stentz, R. S. Windeler, J. L. Hall, and S. T. Cundiff, "Carrier-envelope phase control of femtosecond mode-locked lasers and direct optical frequency synthesis," *Science* **288**(5466), 635–639 (2000).
3. P. B. Corkum and F. Krausz, "Attosecond science," *Nat. Phys.* **3**(6), 381–387 (2007).
4. F. Krausz and M. Ivanov, "Attosecond physics," *Rev. Mod. Phys.* **81**(1), 163–234 (2009).
5. S.-W. Kim, "Metrology: Combs rule," *Nat. Photonics* **3**(6), 313–314 (2009).
6. S. Diddams, "The evolving optical frequency comb," *J. Opt. Soc. Am. B* **27**(11), B51–B62 (2010).
7. N. R. Newbury, "Searching for applications with a fine-tooth comb," *Nat. Photonics* **5**(4), 186–188 (2011).
8. L. Xu, Ch. Spielmann, A. Poppe, T. Brabec, F. Krausz, and T. W. Hänsch, "Route to phase control of ultrashort light pulses," *Opt. Lett.* **21**(24), 2008–2010 (1996).
9. T. Yasui, K. Minoshima, and H. Matsumoto, "Stabilization of femtosecond mode-locked Ti:Sapphire laser for high-accuracy pulse interferometry," *IEEE J. Quantum Electron.* **37**(1), 12–19 (2001).
10. T. R. Schibli, K. Minoshima, F.-L. Hong, H. Inaba, A. Onae, H. Matsumoto, I. Hartl, and M. E. Fermann, "Frequency metrology with a turnkey all-fiber system," *Opt. Lett.* **29**(21), 2467–2469 (2004).
11. I. Hartl, G. Imeshev, M. E. Fermann, C. Langrock, and M. M. Fejer, "Integrated self-referenced frequency-comb laser based on a combination of fiber and waveguide technology," *Opt. Express* **13**(17), 6490–6496 (2005).
12. A. Baltuška, T. Fuji, and T. Kobayashi, "Controlling the carrier-envelope phase of ultrashort light pulses with optical parametric amplifiers," *Phys. Rev. Lett.* **88**(13), 133901 (2002).
13. T. Fuji, J. Rauschenberger, A. Apolonski, V. S. Yakovlev, G. Tempea, T. Udem, C. Gohle, T. W. Hänsch, W. Lehnert, M. Scherer, and F. Krausz, "Monolithic carrier-envelope phase-stabilization scheme," *Opt. Lett.* **30**(3), 332–334 (2005).
14. T. Fuji, A. Apolonski, and F. Krausz, "Self-stabilization of carrier-envelope offset phase by use of difference-frequency generation," *Opt. Lett.* **29**(6), 632–634 (2004).
15. Y. S. Lee, J. H. Sung, C. H. Nam, T. J. Yu, and K.-H. Hong, "Novel method for carrier-envelope-phase stabilization of femtosecond laser pulses," *Opt. Express* **13**(8), 2969–2976 (2005).

16. E. B. Kim, J.-H. Lee, W.-K. Lee, T. T. Luu, and C. H. Nam, "Long-term maintenance of the carrier-envelope phase coherence of a femtosecond laser," *Opt. Express* **18**(25), 26365–26372 (2010).
17. J.-H. Lee, E. B. Kim, T. T. Luu, W.-K. Lee, D.-H. Yu, J. Park, C. Y. Park, T. J. Yu, and C. H. Nam, "Frequency-domain performance of a femtosecond laser with carrier-envelope phase stabilized by the direct locking method," *Appl. Phys. B* **104**(4), 793–797 (2011).
18. S. Koke, C. Grebing, H. Frei, A. Anderson, A. Assion, and G. Steinmeyer, "Direct frequency comb synthesis with arbitrary offset and shot-noise-limited phase noise," *Nat. Photonics* **4**(7), 462–465 (2010).
19. B. Borchers, S. Koke, A. Husakou, J. Herrmann, and G. Steinmeyer, "Carrier-envelope phase stabilization with sub-10 as residual timing jitter," *Opt. Lett.* **36**(21), 4146–4148 (2011).
20. T. Wittmann, B. Horvath, W. Helml, M. G. Schatzel, X. Gu, A. L. Cavalier, G. G. Paulus, and R. Kienberger, "Single-shot carrier-envelope phase measurement of few-cycle laser pulses," *Nat. Phys.* **5**(5), 357–362 (2009).
21. N. G. Johnson, O. Herrwerth, A. Wirth, S. De, I. Ben-Itzhak, M. Lezius, B. Bergues, M. F. Kling, A. Senftleben, C. D. Schröter, R. Moshhammer, J. Ullrich, K. J. Betsch, R. R. Jones, A. M. Saylor, T. Rathje, K. Rühle, W. Müller, and G. G. Paulus, "Single-shot carrier-envelope-phase-tagged ion-momentum imaging of nonsequential double ionization of argon in intense 4-fs laser fields," *Phys. Rev. A* **83**(1), 013412 (2011).
22. M. Kreß, T. Löffler, M. D. Thomson, R. Dörner, H. Gimpel, K. Zrost, T. Ergler, R. Moshhammer, U. Morgner, J. Ullrich, and H. G. Roskos, "Determination of the carrier-envelope phase of few-cycle laser pulses with terahertz-emission spectroscopy," *Nat. Phys.* **2**(5), 327–331 (2006).
23. T. R. Schibli, J. Kim, O. Kuzucu, J. T. Gopinath, S. N. Tandon, G. S. Petrich, L. A. Kolodziejski, J. G. Fujimoto, E. P. Ippen, and F. X. Kaertner, "Attosecond active synchronization of passively mode-locked lasers by balanced cross correlation," *Opt. Lett.* **28**(11), 947–949 (2003).
24. J. Kim, J. Chen, J. Cox, and F. X. Kärtner, "Attosecond-resolution timing jitter characterization of free-running mode-locked lasers," *Opt. Lett.* **32**(24), 3519–3521 (2007).
25. J. Kim, J. A. Cox, J. Chen, and F. X. Kärtner, "Drift-free femtosecond timing synchronization of remote optical and microwave sources," *Nat. Photonics* **2**(12), 733–736 (2008).
26. J. Lee, Y.-J. Kim, K. Lee, S. Lee, and S.-W. Kim, "Time-of-flight measurement with femtosecond light pulses," *Nat. Photonics* **4**(10), 716–720 (2010).
27. J. Lee, K. Lee, S. Lee, S.-W. Kim, and Y.-J. Kim, "High precision laser ranging by time-of-flight measurement of femtosecond pulses," *Meas. Sci. Technol.* **23**(6), 065203 (2012).
28. T.-A. Liu, N. R. Newbury, and I. Coddington, "Sub-micron absolute distance measurements in sub-millisecond times with dual free-running femtosecond Er fiber-lasers," *Opt. Express* **19**(19), 18501–18509 (2011).
29. J. A. Cox, J. Kim, J. Chen, and F. X. Kaertner, "Long-term stable timing distribution of an ultrafast optical pulse train over multiple fiber links with polarization maintaining output," in *Conference on Lasers and Electro-Optics (CLEO), OSA Technical Digest (CD)* (Optical Society of America, 2009), paper CTuS1.
30. J. Kim and F. X. Kaertner, "Attosecond-precision ultrafast photonics," *Laser Photon. Rev.* **4**(3), 432–456 (2010).
31. A. J. Benedick, J. G. Fujimoto, and F. X. Kärtner, "Optical flywheels with attosecond jitter," *Nat. Photonics* **6**(2), 97–100 (2012).

## 1. Introduction

Stabilization of the carrier-envelope phase (CEP) of femtosecond light pulses is required for various applications such as optical frequency metrology [1,2], attosecond physics [3,4], and absolute distance measurements [5–7]. The CEP is the phase slip between the pulse envelope peak and underlying electric-field carrier, which constantly varies when light pulses propagate through a dispersive medium. For stabilization, the CEP needs to be detected at a fast speed for real-time control but this has not been an easy task in the time domain due to the limited CEP detection bandwidth and the ambiguity in carrier phase [8,9]. A breakthrough was found in the frequency domain, instead, by introducing a nonlinear f-2f interferometer [1,2]. Since the first f-2f interferometer was demonstrated in 2000, there have been various reports on different CEP stabilization schemes: common-path geometries with low environmental susceptibility [10,11], nonlinear optical parametric amplification and difference frequency generation for all-optical CEP stabilization [12–14], direct-locking methods without a phase-locked loop [15–17], feed-forward control for quantum-limited performance [18,19], above-threshold ionization for single-shot CEP detection [20,21], and terahertz time-of-flight measurement from the apex of a metal tip [22]. Most of these methods require high pulse energy of more than several nanojoules for nonlinear spectral broadening, wavelength conversion, or ionization of atoms/molecules.

If the envelope and the phase of the femtosecond pulses can be detected separately, the CEP can be controlled in the time domain as well. The interferometric cross-correlation in an unequal-path interferometer is known to provide CEP information by creating interference

between the original and the time-delayed pulses [2,8,9]. Nevertheless, it cannot be used for CEP control, because the unequal-path length must be slowly modulated for CEP detection and it is practically difficult to measure the time difference between the envelope and the carrier at a high update rate. Therefore, a novel detection method that decouples these measurements is essential for real-time CEP control in the time domain.

In this investigation, a time-domain CEP stabilization of femtosecond pulses is demonstrated based on a combination of a balanced optical intensity cross-correlation (BXCOR), and interferometric cross-correlation (IXCOR). Balanced optical cross-correlation optically converts the time difference between two femtosecond pulses into the second harmonic intensity, using only the pulse envelope information, without an electric field carrier. A range of recent BXCOR work has demonstrated this technique's utility in precise timing and length measurements, including the precision timing distribution, synthesis of attosecond pulses, and precision laser ranging [23–27]. Here, the BXCOR is used to lock the unequal path length of an interferometer to an exact integer multiple of the pulse separation. The IXCOR phase measurement is then fed back to stabilize the carrier-envelope phase. The resulting fractional frequency stability of the carrier-envelope-offset frequency,  $f_{ceo}$ , relative to the optical carrier was  $1.18 \times 10^{-11}$  at 0.1 second. The proposed method was confirmed to function with a low pulse energy of about 10 pJ, which is one hundredth of the requirement for conventional f-2f interferometry. This demonstration used relatively long pulses (~800 fs) and one would expect much higher performance from shorter pulses. Finally, note that this technique stabilizes the carrier-envelope offset phase, but does not provide its absolute value. A separate, much lower bandwidth measurement could be used to determine the absolute value of the CEO phase. Alternatively, this technique could be used in applications that require a stable frequency comb tooth position, but not knowledge of the CEO frequency.

## 2. CEP detection methods for femtosecond light pulses

Within a train of femtosecond pulses, as illustrated in Fig. 1(a), the CEP, denoted by  $\varphi$ , represents the relative phase between the optical carrier (solid red line) and the pulse envelope (dotted blue line). The CEP evolves from pulse to pulse when the group velocity of the pulse envelope is not the same as the phase velocity of the optical carrier. CEP phase can be measured from an interferogram between sequential (or further delayed) femtosecond pulses. This can be realized by using an unbalanced interferometer because the temporal coherence of a femtosecond laser repeats at every  $c f_r^{-1}$  (where  $f_r$  is the pulse repetition rate and  $c$  is the speed of light), unlike conventional low-coherent light sources.

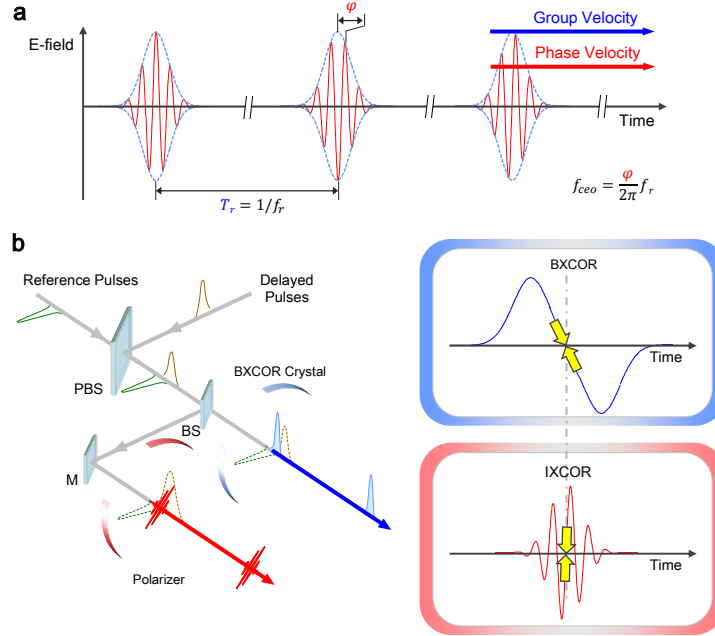


Fig. 1. Time-domain stabilization of femtosecond light pulses. (a) The relative phase between the carrier (solid red line) and the pulse envelope (dotted blue line) evolves from pulse to pulse by the CEP,  $\varphi$  without active stabilization. (b) Detection of the group and phase velocity of femtosecond pulses by optical cross-correlations: BXCOR and IXCOR. Abbreviations are PBS: polarization beam splitter, BS: beam splitter, and M: mirror. Yellow arrows designate lock points.

Figure 1(b) shows the basic concept where a reference and delayed pulse are combined. The BXCOR is used to measure and ultimately stabilize their relative time offset, in this case to  $4 \cdot (cf_r^{-1})$  or 5.80 m. The IXCOR then measures the relative optical phase between the two pulses. In so much as the relative time offset is constant at exactly an integer number of pulse separations, this phase is the carrier-envelope offset phase, which can be fed back and stabilized.

Mathematically, the output pulse train in time is

$$E(t) = e^{-i\omega t} \sum_m e^{im\varphi} e^{i\omega m T_r} a(t - m T_r) \quad (1)$$

where  $\varphi$  is the carrier-envelope offset phase,  $\omega$  is the carrier frequency,  $T_r$  is the pulse separation, and  $a(t)$  is the slowly varying pulse envelope. If the reference and delayed pulse trains are heterodyned against each other with a relative delay of  $t = 4T_r + \tau$ , where  $\tau$  is assumed to be a small timing offset, the resulting detector signal is

$$I(\tau) = I_{AC}(\tau) e^{-i(\omega\tau + 4\varphi)} \quad (2)$$

where  $I_{AC}(\tau)$  is the slowly varying pulse envelope of the interferogram given by the autocorrelation of  $a(t)$ . Assuming a small timing offset, the phase of the interferogram signal is

$$\varphi_{IXCOR} = \omega\tau + 4\varphi + \theta_D \quad (3)$$

where the  $\theta_D$  term was inserted to account for unequal dispersion in the two arms of the interferometer and is ultimately the reason the absolute value of the stabilized CEP is

undetermined. Assuming that  $\theta_D$  is stable, the above equation gives the variations in the CEP as,

$$\delta\varphi = (\omega\delta\tau - \delta\varphi_{IXCOR}) / 4. \quad (4)$$

The BXCOR arm detects  $\delta\tau$  and the IXCOR arm detects  $\varphi_{IXCOR}$ . The BXCOR signal is fed back to the length of the unbalanced interferometer arm to drive  $\delta\tau$  towards zero. The IXCOR signal is fed back to the carrier frequency to drive  $\delta\varphi_{IXCOR}$  towards zero, thereby stabilizing the CEP  $\varphi$ .

### 3. Time-domain CEP stabilization: system configuration

Figure 2 presents the overall experimental apparatus for time-domain CEP stabilization. It is composed of an Er-doped fiber femtosecond laser, an unbalanced interferometer, a balanced intensity cross-correlator, an interferometric cross-correlator, and a performance verification section. The Er-doped fiber femtosecond laser was based on an all-fiber linear cavity design with a saturable absorber mirror (SAM) for high system robustness. It provided ultra-short pulses of 800 femtosecond duration (measured by an auto-correlator) at a 207 MHz repetition rate with an average power of 20 mW [27]. The output wavelength was centered at 1560 nm and had a relatively low 6 nm spectral bandwidth, with could support a minimum temporal width of 600 fs. The repetition rate was locked to the reference clock of a hydrogen maser, by controlling the intra-cavity PZT glued to the cavity fiber. The Allan deviation of the repetition rate was measured at  $2.41 \times 10^{-12}$  at one second averaging.

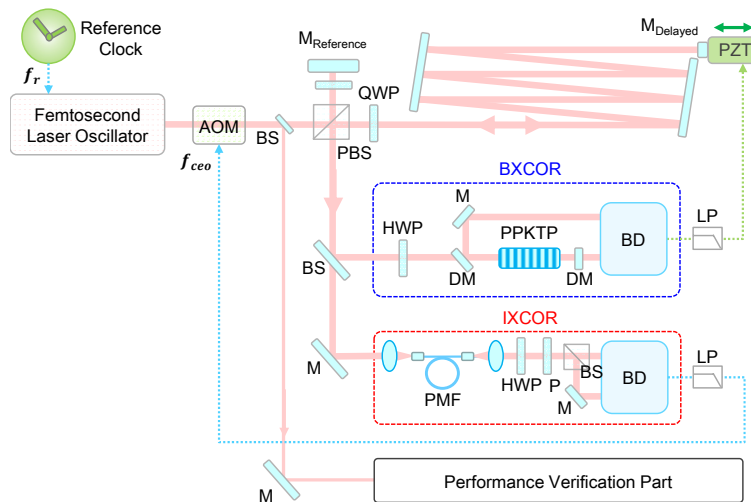


Fig. 2. System layout to stabilize the CEP of an Er-doped fiber femtosecond laser in the time-domain. The time-domain CEP stabilization unit includes an Er-doped femtosecond laser, an unbalanced interferometer, a BXCOR, and an IXCOR. Abbreviations are AOM: acousto-optic modulator, BS: beam splitter, PBS: polarization beam splitter, M: mirror, QWP: quarter-wave plate, PZT: piezo-electric actuator, HWP: half-wave plate, DM: dichroic mirror, PPKTP: periodically poled  $\text{KTiOPO}_4$ , BD: balanced detector, LP: low-pass filter, and PMF: polarization-maintaining fiber.

The output beam from the laser oscillator was split into the reference beam and its time-delayed beam at the polarization beam splitter (PBS); the time-delayed beam propagated a longer optical path than the reference beam by  $4 \cdot (cf_r^{-1})$  in the unbalanced interferometer. These beams were recombined at the PBS. A part of the combined beam was then directed to the BXCOR for pulse-envelope detection, another part directed to the IXCOR in order to detect the optical-phase variation. The relative time delay between the BXCOR and the

IXCOR was adjusted to nearly zero by using the polarization-mode dispersion (PMD) in a polarization maintaining fiber (PMF).

At the BXCOR unit, the temporal offset between the reference and measurement pulses was quantified using a type-II phase-matched PPKTP (periodically poled KTiOPO4) crystal [23–25]. Two second-harmonic (SH) sub-pulses were generated at the crystal (one during the forward propagation and the other during the backward propagation) and they were converted into electrical signals at a balanced photo-detector (Thorlabs PDB 450A at 0.3 MHz bandwidth). The resulting BXCOR signal showed highly linear proportionality to the temporal offset (3.35 mV/fs) between the reference and the time delayed pulses and it became zero when the temporal offset was nullified (See Fig. 3(a)). By using this BXCOR signal, the OPD of the unbalanced interferometer was locked to the pulse repetition rate, which was pre-stabilized as mentioned before. Effectively, both the pulse period and the unbalanced interferometer OPD were locked to the hydrogen maser. The BXCOR signal was confirmed to maintain the locking status with a lower average power down to 2 mW (at the BXCOR part in Fig. 2), which corresponded to  $\sim 10$  pJ at a 207 MHz repetition rate. Therefore, this stabilization scheme can be realized with a femtosecond laser with a low pulse energy without subsequent power amplification.

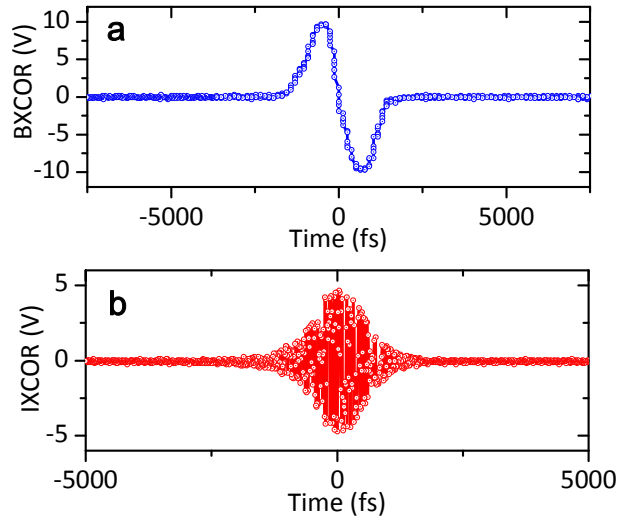


Fig. 3. BXCOR and IXCOR signals while scanning the time delay. (a) BXCOR signal for pulse envelope control. (b) IXCOR signal for carrier electric field control.

The IXCOR was detected at the balanced photo-detector (Thorlabs PDB 150C at 0.3 MHz bandwidth) following the polarizer (See Fig. 3(b)). The slope of the IXCOR signal was 243 mV/femtosecond, which could provide phase jitter of 4 milliradians with a 1 mV noise level. The IXCOR phase was stabilized by feedback to the AOM frequency (see Fig. 2), which shifted the optical frequency of the femtosecond laser within a 4 MHz modulation bandwidth. The injection current to the pump laser diode was tested for the control as well, but the dynamic range and the feedback bandwidth were found to be better when using the AOM.

An in-loop noise analysis was performed for the BXCOR and IXCOR control loops. The time traces of the BXCOR and IXCOR signals were recorded with an oscilloscope while in a locked configuration (See Figs. 4(a-1) and (b-1)). The standard deviations of the BXCOR and IXCOR signals were 0.34 femtosecond and 8.5 mrad, respectively, over 500 s. The power spectral density (PSD) was measured to 2 MHz limited by the sampling rate and the memory size of the oscilloscope, but the current bandwidth included most of the dominant noise sources. Common noise components were observed at 180–300 Hz and were believed to have

arisen by the intensity noise generated by environmental perturbations such as acoustic noise, vibration, and pressure variation. The dominant noise source was the servo bump around 30 kHz and the balanced detector determined the base noise floor at lower frequency regime.

The larger error between these two error contributions determines the CEP stability (see Eq. (3)). Not surprisingly, the largest uncertainty arises from the BXCOR signal, or, in other words, how well the unbalanced interferometer distance is maintained at an exact integer multiple of the pulse repetition length. The 0.34 fs jitter on the BXCOR signal corresponds to a CEP phase jitter of  $(2\pi)(0.34\text{fs})(207\text{THz}) \sim 0.44$  radians at 2 MHz bandwidth. The contribution from the IXCOR signal is below 10 mrad (see Fig. 4(b-2)). Averaged over longer time scales, the timing jitter of the BXCOR signal averages down to  $\sim 4$  attoseconds at 1 second, with a corresponding CEP stability of 5 mrad at 1 second. However, the true CEP noise can be evaluated only through out-of-loop noise measurements.

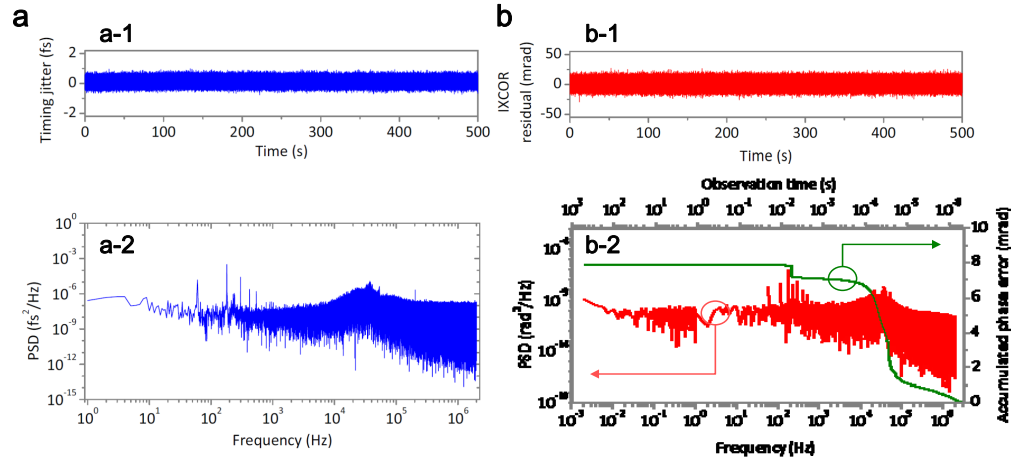


Fig. 4. Measured in-loop timing jitters with BXCOR control; (a-1) time trace and (a-2) spectral density. Measured in-loop optical phase from the IXCOR control; (b-1) time trace, (b-2) spectral density.

#### 4. Experimental results and discussions

In order to verify the stabilization performance, an interferometer CEP-stabilized frequency comb was compared with a cavity-stabilized cw laser as shown in Fig. 5. The stabilized cw laser had a drift of less than 1 Hz per second and its frequency ( $f_{CW}$ ) was measured using a (separate) self-referenced frequency comb. For the purposes of this experiment, the drift and frequency uncertainty of cavity-stabilized cw laser are negligible. The comb-cw heterodyne beat frequency is  $f_b = n f_r + f_{CEO} - f_{CW}$ , where  $n$  is the mode number (See Figs. 5(a) and (b)). Assuming negligible noise on  $f_r$ , which was locked to the H-maser,  $f_b$  can be regarded as a direct measure of  $f_{CEO}$  and compared to the alternative interferometric measurement. We first compared  $f_{CEO}$  to the scaled IXCOR signal,  $f_r \delta \phi_{IXCOR} / 2\pi$  when the unbalanced interferometer is stabilized but the IXCOR phase is free running. (See Fig. 5(c).) This result shows that the proposed time-domain CEP measurement signal has the same variations as  $f_{CEO}$ , as predicted. However, as given in Eq. (2), there is an additional shift that arises from  $\theta_D$ , the differential dispersion in the interferometer, which is fairly constant. Here we measure  $\theta_D$  to be 0.4 radians (using the known cw optical frequency). In principle, after this calibration, the actual  $f_{CEO}$  is known for future measurements (although more observation is needed to evaluate the longterm stability of  $\theta_D$ ).

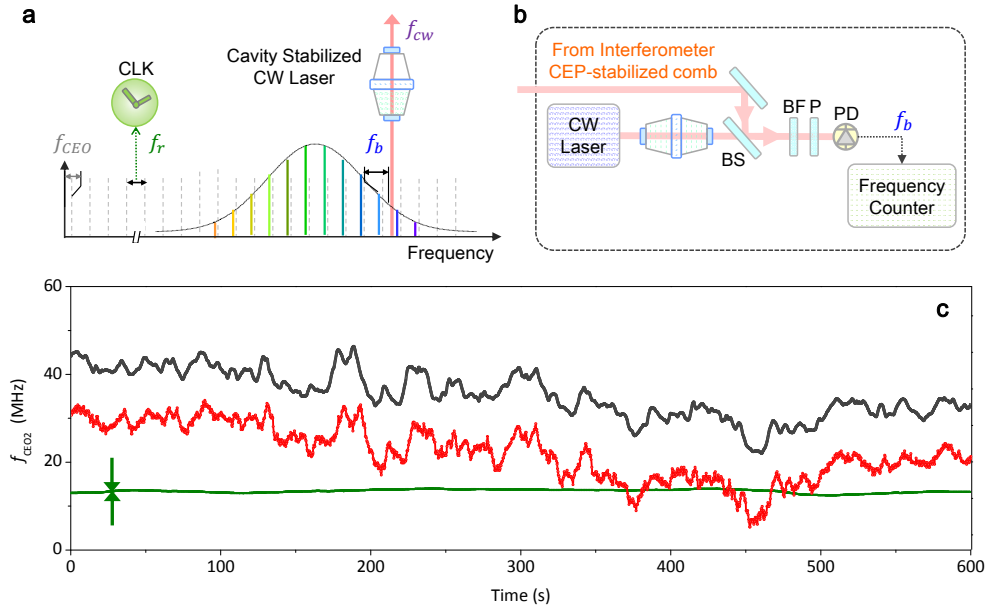


Fig. 5. Comparative measurement between the interferometric stabilized frequency comb and a cavity-stabilized cw reference laser. (a) Schematic of the setup. (b) Experimental configuration. (c) Time variation of the offset frequency measured from the interferometric phase as  $f_r \delta \phi_{IXCOR} / 2\pi$  (red line) and the actual offset frequency measured through the heterodyne signal against the reference cw laser (black line). Green line shows a time trace of locked  $f_{CEO}$  by the proposed method. Abbreviations are BF: bandpass filter, P: polarizer, and PD: photo-detector.

For Fig. 5(c), the frequency-counter gate time of the  $f_{CEO}$  detection was set to 0.1 second and the IXCOR signal was detected at the same update rate for comparison. The update rate of the CEP detection can be increased to more than 100 MHz (whereas the update rate of  $f_{CEO}$  is limited to 1 kHz by the update rate of the frequency counter in use), which is determined by the incident optical power and the electric bandwidth of the balanced detector for the IXCOR: the update rate increases with higher input power and wider detector bandwidth. This potential high update-rate of the CEP detection will be beneficial for real-time CEP tagging in the field of attosecond metrology [21,22].

In the case where the IXCOR phase,  $\phi_{IXCOR}$  is stabilized, the heterodyne beat signal,  $f_b$ , and therefore  $f_{CEO}$  should be constant. The Allan deviation of  $f_b$  under stabilized conditions is shown in Fig. 6. Given the measured stability of the phase lock of  $f_r$ , the residual variations in  $f_b$  are assumed to be due to instability in the  $f_{CEO}$ . Locked stability was evaluated to be  $\sim 50$  times better than the free-running value. Normalized to the optical carrier, the stability, as shown in Fig. 6 was  $1.2 \times 10^{-11}$  at 100 ms,  $5.6 \times 10^{-11}$  at 1 s, and  $4.9 \times 10^{-10}$  at 10 second and saturated at 80 second to  $1.7 \times 10^{-9}$ . While this frequency instability is worse than an  $f$ - $2f$  stabilized system, it is accomplished at much lower pulse energies and without the need for a supercontinuum. Moreover, this level of frequency stability could be readily applied for absolute ranging in ambient air for industrial applications [26–28] or real-time CEP tagging for attosecond metrology where a high update rate is important [21,22].

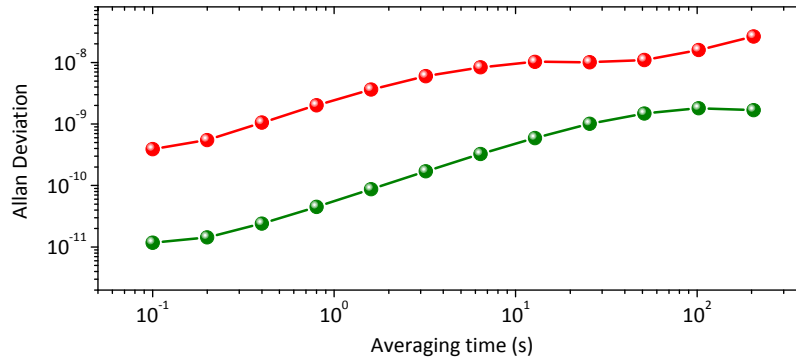


Fig. 6. Allan deviation of the out-of-loop performance of the carrier-envelope offset frequency, normalized to the optical carrier, for the unstabilized frequency comb (red) and with the time-domain CEP stabilization (green).

The CEP instability was, however, one order of magnitude worse than that of the repetition rate at 0.1 second and higher than the value expected in the in-loop noise analysis of Section 3. This difference is thought to originate from the out-of-loop drift of the BXCOR signal, and therefore  $\tau$ , in the current system. Because a relatively long femtosecond pulse of 800 femtosecond ( $\sim 240 \mu\text{m}$  in length) was used for this experiment, out-of-loop timing drift less than the BXCOR detection limit (2.5 nm) could not be compensated [23–25,29,30]. The drift level agreed with the saturated relative CEP stability of  $1.67 \times 10^{-9}$  in Fig. 6, which corresponds to the ratio of this 2.5 nm and the unbalanced OPD of 5.80 m. The current performance could be improved by adopting shorter pulses in order to obtain a steeper BXCOR signal as demonstrated in Ref [31], where hundred-fold steeper BXCOR was demonstrated, or by elongating the unbalanced OPD in order to increase the CEP detection sensitivity.

## 5. Conclusion

In summary, a time-domain CEP stabilization of femtosecond pulses was demonstrated by controlling the pulse envelope and the carrier phase using the BXCOR and IXCOR signals. The proposed CEP stabilization method was confirmed to function with a low pulse energy of  $\sim 10$  pJ without subsequent pulse amplification or spectral broadening. The out-of-loop measurement showed frequency stability of  $1.18 \times 10^{-11}$  at 0.1 second as an Allan deviation. These capabilities could be applied to absolute laser ranging, surface measurements, and real-time CEP tagging.

## Acknowledgments

This work was supported by the Global Research Network Program, the National Space Laboratory (NSL) Program, and the National Honor Scientist Program funded by the National Research Foundation of the Republic of Korea.